



Contents lists available at ScienceDirect

Bioorganic & Medicinal Chemistry

journal homepage: www.elsevier.com/locate/bmc

Synthesis, molecular modeling and biological evaluation of guanidine derivatives as novel antitubulin agents

Yong Qian, Hong-Jia Zhang, Peng-Cheng Lv, Hai-Liang Zhu *

State Key Laboratory of Pharmaceutical Biotechnology, Nanjing University, Nanjing 210093, People's Republic of China

ARTICLE INFO

Article history:

Received 31 August 2010

Revised 2 October 2010

Accepted 5 October 2010

Available online 29 October 2010

Keywords:

Chalcone

Guanidine

Molecular modeling

Antitubulin polymerization

ABSTRACT

A series of novel chalcone guanidine derivatives (**4a–4q**) have been designed and synthesized, and their biological activity were also evaluated as potential antiproliferative and antitubulin polymerization inhibitors. Compound **4q** showed the most potent biological activity ($IC_{50} = 0.09 \pm 0.01 \mu\text{M}$ for MCF-7 and $IC_{50} = 8.4 \pm 0.6 \mu\text{M}$ for tubulin), which is comparable to the positive controls. Docking simulation was performed to position compound **4q** into the colchicine binding site to determine the probable binding model, which suggested probable inhibition mechanism.

Published by Elsevier Ltd.

1. Introduction

Microtubules are key cytoskeletal filaments and play essential roles in numerous cellular functions, such as cell motility, cell division, shape maintenance and vesicle transport. Microtubules are in dynamic equilibrium with tubulin dimers.¹ Inhibiting tubulin polymerization or interfering with microtubule disassembly will interrupt the dynamic equilibrium, leading to cell cycle arrest or cell apoptosis induction. Given their significant role in the cellular functions, microtubule has been a proven molecular target for cancer chemotherapeutic agents. Several natural and synthetic agents capable of interfering with the polymerization or depolymerization of microtubulin have been discovered and currently used in patient.^{2–4} More recently, new tubulin targeting agents have been intensively investigated and developed, such as combretastatin A-4 phosphate, which target the colchicine binding site of the tubulin and disrupt the endothelial cell morphology to stop blood flow through tumor capillaries, and consequently, leading to tumor cell death.^{5–7}

Guanidine derivatives have been intensively reported to possess potent antiviral and anticancer activities.^{8–10} Guanidine derivatives have attracted considerable attention as they have been shown a tendency to inhibit S-adenosylmethionine decarboxylase (SAMDC),¹¹ ribonucleotide reductase (RR),¹² and can accumulate in the mitochondria to damage mitochondrial and inhibit respiratory chain,¹³ and other can bind DNA minor groove,¹⁴ leading to cell proliferation inhibition and apoptosis induction in

the human tumor cells. For example, Methyl-GAG (methylglyoxal-bisguanylhydrazone, MAGA) as a single agent has been used in clinical for malignant lymphoma, carcinoma of the head, neck, and esophageal and non-small-cell lung cancer.¹⁵ Recently, Chen and Cai groups designed and synthesized two series of guanidine analogs as antitubulin polymerization agents which can cause proliferation inhibition and apoptosis induction in tumor models.^{16,17}

As a part of our research for novel antitubulin polymerization agents, we designed and synthesized a series of aminoguanidine analogs based on chalcone scaffold. We chose chalcone moiety as it was an important pharmacophore of natural products and the synthetic precursors that were found to possess various biological activity, including antimetabolic, and antiproliferative activities.^{18,19} Particularly, chalcone derivatives as tubulin binding agents are also explored and developed.²⁰ Herein, we described the synthesis and the SAR of the novel series of guanidine derivatives, and the biological activity evaluation indicated that some of these compounds are potent inhibitors of tubulin polymerization. Docking simulations were also performed using the X-ray crystallographic structure of the tubulin in complex with an inhibitor to explore the binding modes of these compounds at the active site.

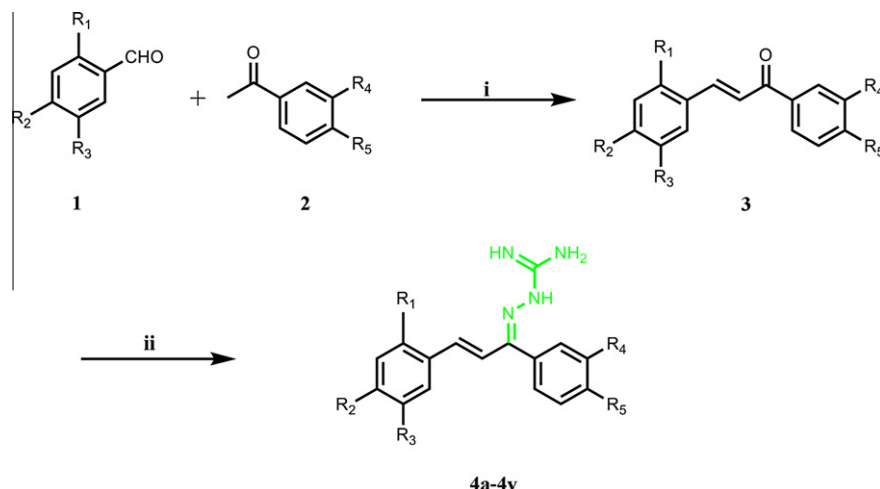
2. Results and discussion

2.1. Chemistry

The synthetic route for the novel aminoguanidine derivatives **4a–4v** is outlined in Scheme 1. These compounds were prepared according to the modified procedure of Fukumoto et al.²¹ by reaction of chalcones with aminoguanidine in the presence of

* Corresponding author. Tel./fax: +86 25 8359 2572.

E-mail address: zhuhl@nju.edu.cn (H.-L. Zhu).



Reagents and conditions: (i). KOH, MeOH, rt; (ii). Aminoguanidine hydrochloride, EtOH, HCl, reflux.

Scheme 1. Synthesis of chalcone aminoguanidine derivatives.

hydrochloric acid with good yields of 70–80%. All the aminoguanidine derivatives were isolated and purified by column chromatography and then recrystallized by acetone/MeOH/Et₂O, and their structure were shown in Table 1. All of the synthetic compounds gave satisfactory analytical and spectroscopia data, which were in full accordance with their depicted structures.

2.2. Biological activity

All the synthesized guanidine compounds **4a–4v** were evaluated for their ability to antiproliferative activities against MCF-7

human breast carcinoma cells. The results were summarized in Table 2. A number of guanidine compounds exhibited remarked effects on antiproliferative activities. Among them, compound **4q** displayed the most potent inhibitory activity ($IC_{50} = 0.09 \pm 0.01 \mu\text{M}$ for MCF-7 and $IC_{50} = 8.4 \pm 0.6 \mu\text{M}$ for tubulin), comparable to the positive control colchicine ($IC_{50} = 0.017 \pm 0.01 \mu\text{M}$ for MCF-7 and $IC_{50} = 3.2 \pm 0.4 \mu\text{M}$ for tubulin, respectively).

Structure–activity relationships in these guanidine derivatives demonstrated that compounds with substitution at the *para* (**4a–4c**, **4e**, and **4f**) position showed more potent activities than those with substitution at the *ortho* (**4l–4o**) and *meta* (**4i–4k**) position in the A-ring. A comparison of the *para* position substitution on the A-ring demonstrated that a *para* halogen group (**4a–4c**) have slightly improved antiproliferative activity and the potency order is $F < Cl < Br$, whereas a methyl (**4g**) and methoxy (**4h**) group

Table 1
Structure of chalcone aminoguanidine derivatives

Compound	R ₁	R ₂	R ₃	R ₄	R ₅
4a	H	F	H	H	H
4b	H	Cl	H	H	H
4c	H	Br	H	H	H
4d	H	H	H	H	H
4e	H	Ph	H	H	H
4l	H	OCH ₂ Ph	H	H	H
4g	H	Me	H	H	H
4h	H	OMe	H	H	H
4i	H	H	NO ₂	H	H
4j	H	H	F	H	H
4k	H	H	OMe	H	H
4l	F	H	H	H	H
4m	Cl	H	H	H	H
4n	Br	H	H	H	H
4o	OMe	H	H	H	H
4p	H	H	H	H	Cl
4q	H	H	H	H	Br
4r	H	H	H	H	Me
4s	H	H	H	H	OMe
4t	H	H	H	H	Cl
4u	Cl	H	H	H	OMe
4v	A ring =			H	H

Table 2
Inhibition of tubulin polymerization and inhibition (IC_{50}) of MCF-7 cells proliferation by compound **4a–4v**

Compound	MCF-7 ^a $IC_{50} \pm SD$ (μM)	Tubulin ^b $IC_{50} \pm SD$ (μM)
4a	2.5 ± 0.12	28 ± 4
4b	0.7 ± 0.1	14 ± 2
4c	0.25 ± 0.04	10 ± 3
4d	17 ± 2	140 ± 40
4e	0.8 ± 0.05	12 ± 3
4f	1.2 ± 0.02	16 ± 2
4g	16 ± 4	170 ± 30
4h	14 ± 2	140 ± 20
4i	6.5 ± 0.7	85 ± 8
4j	16 ± 3	150 ± 20
4k	13 ± 3	130 ± 40
4l	3.9 ± 0.15	42 ± 5
4m	4.2 ± 0.45	55 ± 10
4n	4.2 ± 0.5	52 ± 8
4o	7.2 ± 0.6	84 ± 7
4p	0.35 ± 0.04	15 ± 4
4q	0.09 ± 0.01	8.4 ± 0.6
4r	14 ± 3	150 ± 20
4s	13 ± 2	130 ± 15
4t	1.9 ± 0.7	24 ± 6
4u	8.1 ± 0.4	80 ± 10
4v	1.6 ± 0.2	18 ± 3
Colchicine	0.017 ± 0.01	3.2 ± 0.4
CSA-4	0.013 ± 0.003	2.2 ± 0.2

^a Inhibition the growth of MCF-7 human breast carcinoma cells.

^b Inhibition of tubulin polymerization.

substituent had minimal effects compared with **4d**. Meanwhile, a significant loss of activity was observed when the halogen substituent was moved from the *para* position to the *ortho* (**4j**) or *meta* (**4l–4n**) position in the A-ring. A methoxy group at *para* (**4h**), *meta* (**4k**), and *ortho* (**4o**) in the A-ring all led to a noteworthy poor activity. Considering the steric effect of the A-ring, we designed and evaluated the compounds with *p*-phenyl (**4e**), *p*-benzyloxy (**4f**) group substituent in the A-ring, moreover, variation of the aromatic A-ring with a naphthyl moiety substituent (**4v**), which all exhibited good antiproliferative activity. The compounds with *para* halogen substituted (**4p**, **4q**) in the B-ring exhibited excellent antiproliferative activity, **4q** with substituent of *p*-Br showed the most potent activity in these compounds. However, compound **4r** (*p*-Me) and **4s** (*p*-OMe) displayed a poor activity. Interesting, compound **4t** (with 3,4-Cl group in the B-ring) and compound **4u** (with a *p*-Cl group in the A-ring and a *p*-OMe group in the B-ring) also showed the moderate activity.

To examine whether the compounds interact with tubulin and inhibit tubulin polymerization in vitro, we performed the tubulin assembly assay. As shown in Table 2, compounds **4c**, **4e**, and **4q** showed strong inhibitory effect and their 50% tubulin polymerization inhibition about $10 \pm 3 \mu\text{M}$, $12 \pm 4 \mu\text{M}$, and $8.4 \pm 0.6 \mu\text{M}$, respectively. Compound **4q** displayed the most potent antitubulin polymerization activity. The result confirmed that the antiproliferative effect was mediated by direct interaction of compounds with tubulin.

To further address the death pattern, the effect of compound **4q** on the morphology of MCF-7 human breast carcinoma cells was further tested using the fluorescent nuclear DNA stain DAPI, which is sensitive to DNA. Results of DAPI staining assay showed that cells demonstrated apoptotic features, including chromatin aggregation, nuclear and cytoplasmic condensation, nuclear fragmentation, and nucleus into membrane bound vesicles (apoptotic bodies) after treatment with the compound **4q** for 24 h. (Fig. 2)

Compound **4q** was also performed cell cycle analysis using flow cytometry. Cell cycle analysis (Fig. 3) showed that the compound **4q** strongly induced G2/M arrest in MCF-7 cells, and this effect was observed in a dose-independent manner after treatment for 24 h increasing amounts of the compound **4q** (treatment with 50 nm and 500 nm, respectively). About 54.12% of the cells were arrested in the G2/M phase after treatment with 500 nM **4q** for 24 h. These findings indicated a continuing impairment of cell division and confirmed compound **4q** was a potent antitubulin agent.

In order to gain more understanding of the structure–activity relationships observed at the tubulin, molecular docking of the most potent inhibitor **4q** into the colchicine binding site of tubulin was performed on the binding model based on the tubulin structure (PDB code: 1SA0). The binding model of compound **4q** and tubulin is depicted in Figures 4A and B. In the binding model, compound **4q** is nicely bound to the colchicine site of tubulin via hydrogen bond with THR 179 (angle $\text{O}\cdots\text{H}-\text{N} = 146.729^\circ$, distance = 2.249 Å), ASN 349 (angle $\text{O}\cdots\text{H}-\text{N} = 161.980^\circ$, distance = 1.584 Å). As depicted in Figure 2B, more details revealed that the hydrophobic pockets of binding site were also occupied by compound **4q**. The bromophenyl moiety of B-ring occupied a pocket bounded by LEU 248, ALA 250 and LEU 255, the phenyl moiety of A-ring was embedded in a hydrophobic pocket constructed by the residues of SER 178 and LYS 352. The assay data and the molecular docking results showed that compound **4q** was a potential antitubulin inhibitor.

3. Conclusions

A series of chalcone-type guanidine compounds have been designed and synthesized, and their biological activities were also

evaluated as potent antitubulin polymerization inhibitors and antiproliferative activity against MCF-7 human breast carcinoma cells. Compound **4q** demonstrated the most potent inhibitory activity that inhibited the growth of MCF-7 cells with IC_{50} of $0.09 \pm 0.01 \mu\text{M}$ and inhibited the polymerization of tubulin with IC_{50} of $8.4 \pm 0.6 \mu\text{M}$, which was compared with the positive control. Docking simulation was performed to study the probable binding model. Analysis of the compound **4q**'s binding conformation in the colchicine binding site demonstrated that compound **4q** was stabilized by hydrogen bonding interaction with THR 179 and ASN 349. Moreover, the binding of compound **4q** to tubulin was also stabilized by hydrophobic interaction. Antitubulin polymerization and antiproliferative assay results showed the compound **4q** was a potential anticancer agent.

4. Experiments

4.1. Materials and measurements

All chemicals and reagents used in current study were of analytical grade. All the ^1H NMR spectra were recorded on a Bruker DRX 500 or DPX 300 model Spectrometer in CDCl_3 or $\text{DMSO}-d_6$ and chemical shifts was reported in ppm (δ). ESI-MS spectra were recorded on a Mariner System 5304 Mass spectrometer. Elemental analyzes were performed on a CHN-O-Rapid instrument. TLC was performed on the glass-backed silica gel sheets (silica gel 60 Å GF254) and visualized in UV light (254 nm). Column chromatography was performed using silica gel (200–300 mesh) eluting with ethyl acetate and petroleum ether.

4.2. General procedure for synthesis of chalcones

To a stirred solution of acetophenone derivatives or acetone (1 mmol) and a benzaldehyde derivatives (1 mmol) in MeOH (30 mL) was added 6 M KOH (4 mL) and the reaction mixture was stirred until the solids formed. The products were filtrated and washed carefully with ice water and cool MeOH; the resulting chalcones were purified by crystallization from MeOH in refrigerator. (Scheme 1)

4.3. General procedure for the preparation of aminoguanidine derivatives of chalcones

Chalcone (1 mmol), aminoguanidine hydrochloride (1 mmol) and concentrated HCl (0.2 mL) in EtOH (6 mL) were refluxed for 24 h. The solvent was evaporated under reduced pressure. The residue was washed by water several times, then washed by Et_2O , and the residue was purified by column chromatography and then recrystallized by acetone/MeOH/ Et_2O to give the compounds (**4a–4x**). (Scheme 1)

4.3.1. 2-(3-(4-Fluorophenyl)-1-phenylallylidene)hydrazinecarboximidamide (**4a**)

^1H NMR (500 MHz, $\text{DMSO}-d_6$, δ ppm): 6.87(d, $J = 16.0$ Hz, 1H, $-\text{CH}=\text{}$), 7.24 (t, $J = 8.5$ Hz 2H, ArH), 7.46–7.48 (m, 3H, ArH), 7.62 (d, $J = 16$ Hz, 1H, $-\text{CH}=\text{}$), 7.63–7.66 (m, 2H, ArH), 7.77 (br s, 3H), 7.86 (dd, $J = 6.0, 8.0$ Hz, 2H, ArH), 11.9 (s, 1H). ESI-MS: 283.1 ($\text{C}_{16}\text{H}_{16}\text{FN}_4$, $[\text{M}+\text{H}]^+$). Anal. Calcd for $\text{C}_{16}\text{H}_{15}\text{FN}_4$: C, 68.07%; H, 5.36%; N, 19.85%. Found: C, 68.38%; H, 5.79%; N, 20.17%.

4.3.2. 2-(3-(4-Chlorophenyl)-1-phenylallylidene)hydrazinecarboximidamide (**4b**)

^1H NMR (500 MHz, CDCl_3 , δ ppm): 3.49 (s, 1H), 6.37 (d, $J = 16$ Hz, 1H, $-\text{CH}=\text{}$), 6.39 (br s, 1H), 7.07 (d, $J = 16$ Hz, 1H, $-\text{CH}=\text{}$), 7.24–7.25 (m, 2H, ArH), 7.29–7.34 (m, 4H, ArH), 7.58–7.59 (m, 3H, ArH), 7.95

(br s, 1H), 10.09 (s, 1H). ESI-MS: 299.1 (C₁₆H₁₆ClN₄, [M+H]⁺). Anal. Calcd for C₁₆H₁₅ClN₄: C, 64.32%; H, 5.06%; N, 18.75%. Found: C, 64.68%; H, 5.41%; N, 19.12%.

4.3.3. 2-(3-(4-Bromophenyl)-1-phenylallylidene)hydrazinecarboximidamide (4c)

¹H NMR (300 MHz, CDCl₃, δ ppm): 2.49 (s, 1H), 6.34 (s, 1H), 6.36 (d, J = 16.3 Hz, 1H, -CH=), 7.04 (d, J = 16.3 Hz, 1H, -CH=), 7.23–7.51 (m, 6H), 7.51–7.70 (m, 4H), 8.53 (s, 1H). ESI-MS: 343.0 (C₁₆H₁₆BrN₄, [M+H]⁺). Anal. Calcd for C₁₆H₁₅BrN₄: C, 55.99%; H, 4.41%; N, 16.32%. Found: C, 56.35%; H, 4.73%; N, 16.67%.

4.3.4. 2-(1,3-Diphenylallylidene)hydrazinecarboximidamide (4d)

¹H NMR (500 MHz, CDCl₃, δ ppm): 6.33 (br s, 1H), 6.85 (d, J = 16.0 Hz, 1H, -CH=), 7.29–7.36 (m, 5H, ArH), 7.52–7.57 (m, 3H, ArH), 7.62 (d, J = 16.0 Hz, 1H, -CH=), 7.69 (d, J = 7.0 Hz, 2H, ArH), 7.83 (br s, 2H), 11.63 (br s, 1H). ESI-MS: 265.1 (C₁₆H₁₇N₄, [M+H]⁺). Anal. Calcd for C₁₆H₁₆N₄: C, 72.70%; H, 6.10%; N, 21.20%. Found: C, 72.95%; H, 6.43%; N, 21.51%.

4.3.5. 2-(3-(Biphenyl-4-yl)-1-phenylallylidene)hydrazinecarboximidamide (4e)

¹H NMR (500 MHz, CDCl₃, δ ppm): 6.41 (br s, 1H), 6.84 (d, J = 16.0 Hz, 1H, -CH=), 7.33 (d, J = 7.5 Hz, 1H, ArH), 7.37–7.42 (m, 4H, ArH), 7.46–7.54 (m, 7H, ArH), 7.67 (d, J = 16.0 Hz, 1H, -CH=), 7.74 (d, J = 8.5 Hz, 2H, ArH), 7.93 (br s, 1H), 8.03 (br s, 1H), 11.67 (br s, 1H). ESI-MS: 341.2 (C₂₂H₂₁N₄, [M+H]⁺). Anal. Calcd for C₂₂H₂₀N₄: C, 77.62%; H, 5.92%; N, 16.46%. Found: C, 77.91%; H, 6.27%; N, 16.71%.

4.3.6. 2-(3-(4-(Benzyloxy)phenyl)-1-phenylallylidene)hydrazinecarboximidamide (4f)

¹H NMR (500 MHz, CDCl₃, δ ppm): 5.07 (s, 2H, -CH₂-), 6.37 (d, J = 16.0 Hz, 1H, -CH=), 6.43 (br s, 1H), 6.93 (d, J = 8.5 Hz, 1H, ArH), 6.97 (d, J = 16.0 Hz, 1H, -CH=), 7.24–7.25 (m, 3H, ArH), 7.33–7.35 (m, 3H, ArH), 7.38–7.43 (m, 4H, ArH), 7.56–7.57 (m, 3H, ArH), 7.91 (br s, 3H). ESI-MS: 371.2 (C₂₃H₂₃N₄O, [M+H]⁺). Anal. Calcd for C₂₃H₂₂N₄O: C, 74.57%; H, 5.99%; N, 15.12%. Found: C, 74.93%; H, 6.37%; N, 15.45%.

4.3.7. 2-(1-Phenyl-3-p-tolylallylidene)hydrazinecarboximidamide (4g)

¹H NMR (500 MHz, CDCl₃, δ ppm): 2.31 (s, 3H, -CH₃), 6.33 (br s, 1H), 6.82 (d, J = 15.5 Hz, 1H, -CH=), 7.12–7.15 (m, 3H, ArH), 7.28 (d, J = 7.0 Hz, 1H, ArH), 7.45 (d, J = 5.0 Hz, 2H, ArH), 7.52–7.53 (m, 4H, ArH), 7.81 (br s, 2H), 11.61 (s, 1H). ESI-MS: 279.2 (C₁₇H₁₉N₄, [M+H]⁺). Anal. Calcd for C₁₇H₁₈N₄: C, 73.35%; H, 6.52%; N, 20.13%. Found: C, 73.69%; H, 6.88%; N, 20.47%.

4.3.8. 2-(3-(4-Methoxyphenyl)-1-phenylallylidene) hydrazinecarboximidamide (4h)

¹H NMR (300 MHz, DMSO-d₆, δ ppm): 3.79 (s, 1H, -OCH₃), 6.79 (d, J = 9.6 Hz, 1H, -CH=), 6.96 (d, J = 5.4 Hz, 2H, ArH), 7.47–7.49 (m, 3H, ArH), 7.62–7.64 (m, 3H), 7.75–7.79 (m, 5H), 12.0 (s, 1H). ESI-MS: 295.1 (C₁₇H₁₉N₄O, [M+H]⁺). Anal. Calcd for C₁₇H₁₈N₄O: C, 69.37%; H, 6.16%; N, 19.03%. Found: C, 69.68%; H, 6.49%; N, 19.40%.

4.3.9. 2-(3-(3-Nitrophenyl)-1-phenylallylidene) hydrazinecarboximidamide (4i)

¹H NMR (500 MHz, DMSO-d₆, δ ppm): 7.06 (d, J = 16.0 Hz, 1H, -CH=), 7.47–7.50 (m, 3H, ArH), 7.69–7.79 (m, 4H, ArH), 7.77–7.79 (br s, 3H), 8.21 (d, J = 8.5 Hz, 1H, ArH), 8.32 (d, J = 7.0 Hz, 1H, ArH), 8.57 (s, 1H), 11.8 (s, 1H). ESI-MS: 310.3 (C₁₆H₁₆N₅O₂, [M+H]⁺). Anal. Calcd for C₁₆H₁₅N₅O₂: C, 62.13%; H, 4.89%; N, 22.64%. Found: C, 62.49%; H, 5.23%; N, 22.91%.

4.3.10. 2-(3-(3-Fluorophenyl)-1-phenylallylidene)hydrazinecarboximidamide (4j)

¹H NMR (500 MHz, CDCl₃, δ ppm): 6.38 (d, J = 16.0 Hz, 1H, -CH=), 6.52 (br s, 1H), 6.99 (t, J = 6.5 Hz, 1H, ArH), 7.05–7.15 (m, 3H), 7.24–7.31 (m, 3H, ArH), 7.42–7.61 (m, 4H), 7.93 (br s, 2H). ESI-MS: 283.1 (C₁₆H₁₆FN₄, [M+H]⁺). Anal. Calcd for C₁₆H₁₅FN₄: C, 68.07%; H, 5.36%; N, 19.85%. Found: C, 68.38%; H, 5.79%; N, 20.17%.

4.3.11. 2-(3-(3-Methoxyphenyl)-1-phenylallylidene)hydrazinecarboximidamide (4k)

¹H NMR (500 MHz, CDCl₃, δ ppm): 3.88 (s, 3H, -OCH₃), 6.36 (br s, 1H), 6.85 (d, J = 16.0 Hz, 1H, -CH=), 6.96 (d, J = 8.5 Hz, 2H, ArH), 7.28–7.34 (m, 5H, ArH), 7.50 (d, J = 8.5 Hz, 2H, ArH), 7.54 (d, J = 16.0 Hz, 1H, -CH=), 7.82 (br s, 2H), 7.99 (br s, 1H). ESI-MS: 295.1 (C₁₇H₁₉N₄O, [M+H]⁺). Anal. Calcd for C₁₇H₁₈N₄O: C, 69.37%; H, 6.16%; N, 19.03%. Found: C, 69.42%; H, 6.49%; N, 19.33%.

4.3.12. 2-(3-(2-Fluorophenyl)-1-phenylallylidene)hydrazinecarboximidamide (4l)

¹H NMR (500 MHz, CDCl₃, δ ppm): 6.41 (br s, 1H), 6.84 (d, J = 15.5 Hz, 1H, -CH=), 7.20–7.35 (m, 5H, ArH), 7.43–7.55 (m, 3H, ArH), 7.57–7.59 (m, 2H), 7.84 (br s, 2H), 11.64 (br s, 1H). ESI-MS: 283.1 (C₁₆H₁₆FN₄, [M+H]⁺). Anal. Calcd for C₁₆H₁₅FN₄: C, 68.07%; H, 5.36%; N, 19.85%. Found: C, 68.42%; H, 5.69%; N, 20.16%.

4.3.13. 2-(3-(2-Chlorophenyl)-1-phenylallylidene)hydrazinecarboximidamide (4m)

¹H NMR (300 MHz, CDCl₃, δ ppm): 6.32 (br s, 1H), 6.88 (d, J = 16.3 Hz, 1H, -CH=), 7.03 (d, J = 16.3 Hz, 1H, -CH=), 7.22–7.35 (m, 4H, ArH), 7.51 (s, 2H), 7.56–7.70 (m, 5H, ArH), 8.59 (br s, 1H). ESI-MS: 299.1 (C₁₆H₁₆ClN₄, [M+H]⁺). Anal. Calcd for C₁₆H₁₅ClN₄: C, 64.32%; H, 5.06%; N, 18.75%. Found: C, 64.68%; H, 5.37%; N, 19.07%.

4.3.14. 2-(3-(2-Bromophenyl)-1-phenylallylidene)hydrazinecarboximidamide (4n)

¹H NMR (500 MHz, CDCl₃, δ ppm): 6.40 (br s, 1H), 6.82 (d, J = 16.0 Hz, 1H, -CH=), 7.02 (d, J = 16.0 Hz, 1H, -CH=), 7.12–7.17 (m, 1H, ArH), 7.28–7.34 (m, 3H, ArH), 7.45–7.63 (m, 5H, ArH), 7.85 (br s, 2H), 11.65 (br s, 1H). ESI-MS: 343.0 (C₁₆H₁₆BrN₄, [M+H]⁺). Anal. Calcd for C₁₆H₁₅BrN₄: C, 55.99%; H, 4.41%; N, 16.32%. Found: C, 56.32%; H, 4.79%; N, 16.68%.

4.3.15. 2-(3-(2-Methoxyphenyl)-1-phenylallylidene)hydrazinecarboximidamide (4o)

¹H NMR (500 MHz, CDCl₃, δ ppm): 3.38 (s, 3H, -OCH₃), 6.41 (br s, 1H), 6.70 (d, J = 16.5 Hz, 1H, -CH=), 6.88–6.97 (m, 2H, ArH), 7.13 (d, J = 16.5 Hz, 1H, -CH=), 7.21–7.28 (m, 2H, ArH), 7.45–7.51 (m, 5H, ArH), 7.74 (br s, 2H), 11.48 (br s, 1H). ESI-MS: 295.1 (C₁₇H₁₉N₄O, [M+H]⁺). Anal. Calcd for C₁₇H₁₈N₄O: C, 69.37%; H, 6.16%; N, 19.03%. Found: C, 69.98%; H, 6.51%; N, 19.37%.

4.3.16. 2-(1-(4-Chlorophenyl)-3-phenylallylidene) hydrazinecarboximidamide (4p)

¹H NMR (300 MHz, DMSO-d₆, δ ppm): 6.88 (d, J = 9.6 Hz, 1H, -CH=), 7.39–7.44 (m, 3H, ArH), 7.53–7.55 (m, 2H, ArH), 7.64 (d, J = 9.6 Hz, 1H, -CH=), 7.71–7.80 (m, 7H), 11.83 (br s, 1H). ESI-MS: 299.1 (C₁₆H₁₆ClN₄, [M+H]⁺). Anal. Calcd for C₁₆H₁₅ClN₄: C, 64.32%; H, 5.06%; N, 18.75%. Found: C, 64.71%; H, 5.42%; N, 19.10%.

4.3.17. 2-(1-(4-Bromophenyl)-3-phenylallylidene)hydrazinecarboximidamide (4q)

¹H NMR (300 MHz, DMSO-d₆, δ ppm): 6.88 (d, J = 16.3 Hz, 1H, -CH=), 7.32–7.43 (m, 3H), 7.47–7.53 (m, 1H), 7.62–7.72 (m, 4H), 7.80–7.85 (m, 5H), 12.05 (s, 1H). ESI-MS: 343.0 (C₁₆H₁₆BrN₄, [M+H]⁺). Anal. Calcd for C₁₆H₁₅BrN₄: C, 55.99%; H, 4.41%; N, 16.32%. Found: C, 56.31%; H, 4.78%; N, 16.65%.

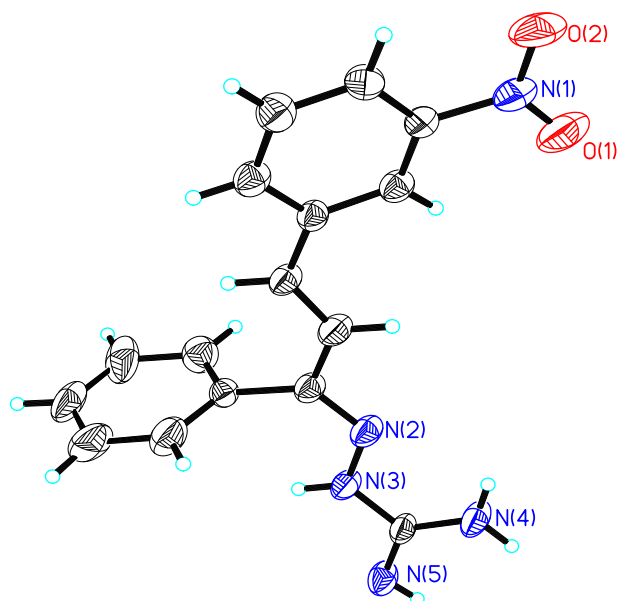


Figure 1. Crystal structure diagrams of compound **4i**. Molecule structure diagram with displacement ellipsoids being at the 30% probability level and H atoms are shown as small spheres of arbitrary radii (Cl anion is omitted for clarity).

4.3.18. 2-(3-Phenyl-1-p-tolylallylidene)hydrazinecarboximidamide (**4r**)

$^1\text{H NMR}$ (500 MHz, CDCl_3 , δ ppm): 2.44 (s, 3H, $-\text{CH}_3$), 6.40 (br s, 1H), 7.09 (d, $J = 16.5$ Hz, 1H, $-\text{CH}=\text{}$), 7.14 (d, $J = 7.5$ Hz, 2H, ArH), 7.31–7.41 (m, 7H, ArH), 7.46 (d, $J = 16.5$ Hz, 1H, $-\text{CH}=\text{}$), 7.78 (br s, 1H), 8.04 (br s, 1H), 10.12 (br s, 1H). ESI-MS: 279.2 ($\text{C}_{17}\text{H}_{19}\text{N}_4$, $[\text{M}+\text{H}]^+$). Anal. Calcd for $\text{C}_{17}\text{H}_{18}\text{N}_4$: C, 73.35%; H, 6.52%; N, 20.13%. Found: C, 73.63%; H, 6.81%; N, 20.50%.

4.3.19. 2-(1-(4-Methoxyphenyl)-3-phenylallylidene)hydrazinecarboximidamide (**4s**)

$^1\text{H NMR}$ (500 MHz, CDCl_3 , δ ppm): 3.89 (s, 3H, $-\text{OCH}_3$), 6.35 (br s, 1H), 6.87 (d, $J = 15.5$ Hz, 1H, $-\text{CH}=\text{}$), 6.97 (d, $J = 8.0$ Hz, 1H, ArH), 7.10 (d, $J = 16.5$ Hz, 1H, ArH), 7.33–7.36 (m, 2H, ArH), 7.44–7.45 (m, 1H, ArH), 7.51–7.52 (m, 2H, ArH), 7.67–7.71 (m, 2H, ArH), 7.82 (br s, 1H), 7.83 (d, $J = 15.5$ Hz, 1H, $-\text{CH}=\text{}$), 11.55 (br s, 1H). ESI-MS:

295.1 ($\text{C}_{17}\text{H}_{19}\text{N}_4\text{O}$, $[\text{M}+\text{H}]^+$). Anal. Calcd for $\text{C}_{17}\text{H}_{18}\text{N}_4\text{O}$: C, 69.37%; H, 6.16%; N, 19.03%. Found: C, 69.68%; H, 6.49%; N, 19.40%.

4.3.20. 2-(1-(3,4-Dichlorophenyl)-3-phenylallylidene)hydrazinecarboximidamide (**4t**)

$^1\text{H NMR}$ (500 MHz, CDCl_3 , δ ppm): 6.39 (br s, 1H), 6.75 (d, $J = 15.0$ Hz, 1H, $-\text{CH}=\text{}$), 7.40 (d, $J = 8.0$ Hz, 1H, ArH), 7.52–8.05 (m, 8H), 8.16 (br s, 1H), 8.73 (br s, 2H). ESI-MS: 332.1 ($\text{C}_{16}\text{H}_{15}\text{Cl}_2\text{N}_4$, $[\text{M}+\text{H}]^+$). Anal. Calcd for $\text{C}_{16}\text{H}_{14}\text{Cl}_2\text{N}_4$: C, 57.67%; H, 4.23%; N, 16.81%. Found: C, 57.93%; H, 4.58%; N, 17.16%.

4.3.21. 2-(3-(2-Chlorophenyl)-1-(4-methoxyphenyl)allylidene)hydrazinecarboximidamide (**4u**)

$^1\text{H NMR}$ (300 MHz, CDCl_3 , δ ppm): 3.90 (s, 3H, $-\text{OCH}_3$), 6.35 (br s, 1H), 6.90–6.99 (m, 2H), 7.05–7.11 (m, 2H), 7.21–7.26 (m, 4H), 7.32–7.36 (m, 3H), 7.62–7.65 (m, 1H), 8.65 (s, 1H). ESI-MS: 329.1 ($\text{C}_{17}\text{H}_{18}\text{ClN}_4\text{O}$, $[\text{M}+\text{H}]^+$). Anal. Calcd for $\text{C}_{17}\text{H}_{17}\text{ClN}_4\text{O}$: C, 62.10%; H, 5.21%; N, 17.04%. Found: C, 62.43%; H, 5.58%; N, 17.31%.

4.3.22. 2-(3-(Naphthalen-2-yl)-1-phenylallylidene)hydrazinecarboximidamide (**4v**)

$^1\text{H NMR}$ (500 MHz, CDCl_3 , δ ppm): 6.36 (br s, 1H), 7.41–7.49 (m, 4H), 7.51 (d, $J = 7.5$ Hz, 2H, ArH), 7.54 (d, $J = 7.0$ Hz, 1H, ArH), 7.60 (d, $J = 6.5$ Hz, 2H, ArH), 7.65 (d, $J = 9.5$ Hz, 1H, ArH), 7.73–7.79 (m, 3H), 8.43 (d, $J = 7.5$ Hz, 1H, ArH), 7.70 (br s, 3H), 11.69 (s, 1H). ESI-MS: 315.2 ($\text{C}_{20}\text{H}_{19}\text{N}_4$, $[\text{M}+\text{H}]^+$). Anal. Calcd for $\text{C}_{20}\text{H}_{18}\text{N}_4$: C, 76.41%; H, 5.77%; N, 19.40%. Found: C, 76.72%; H, 6.08%; N, 19.73%.

4.4. Crystal structure determination

Crystal structure determination of compound **4i** were carried out on a Nonius CAD4 diffractometer equipped with graphite-monochromated $\text{MoK}\alpha$ ($\lambda = 0.71073$ Å) radiation (Fig. 1). The structure was solved by direct methods and refined on F^2 by full-matrix least-squares methods using SHELX-97.²² All the non-hydrogen atoms were refined anisotropically. All the hydrogen atoms were placed in calculated positions and were assigned fixed isotropic thermal parameters at 1.2 times the equivalent isotropic U of the atoms to which they are attached and allowed to ride on their respective parent atoms. The contributions of these hydrogen atoms were included in the structure-factors calculations. The crystal data, data collection, and refinement parameter for the compound **4i** are listed in Table 3.

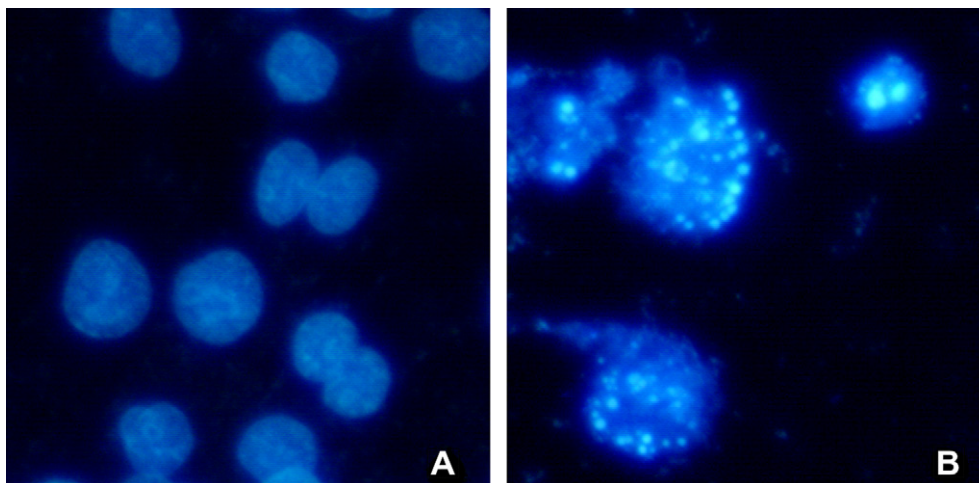


Figure 2. The morphological changes of DAPI-stained MCF-7 human breast carcinoma cells after treatment with compound **4q** (1.0 μM) as observed under a fluorescent microscope. (A) cells were treated without the compound; (B) cells were treated with the compound at 1.0 μM .

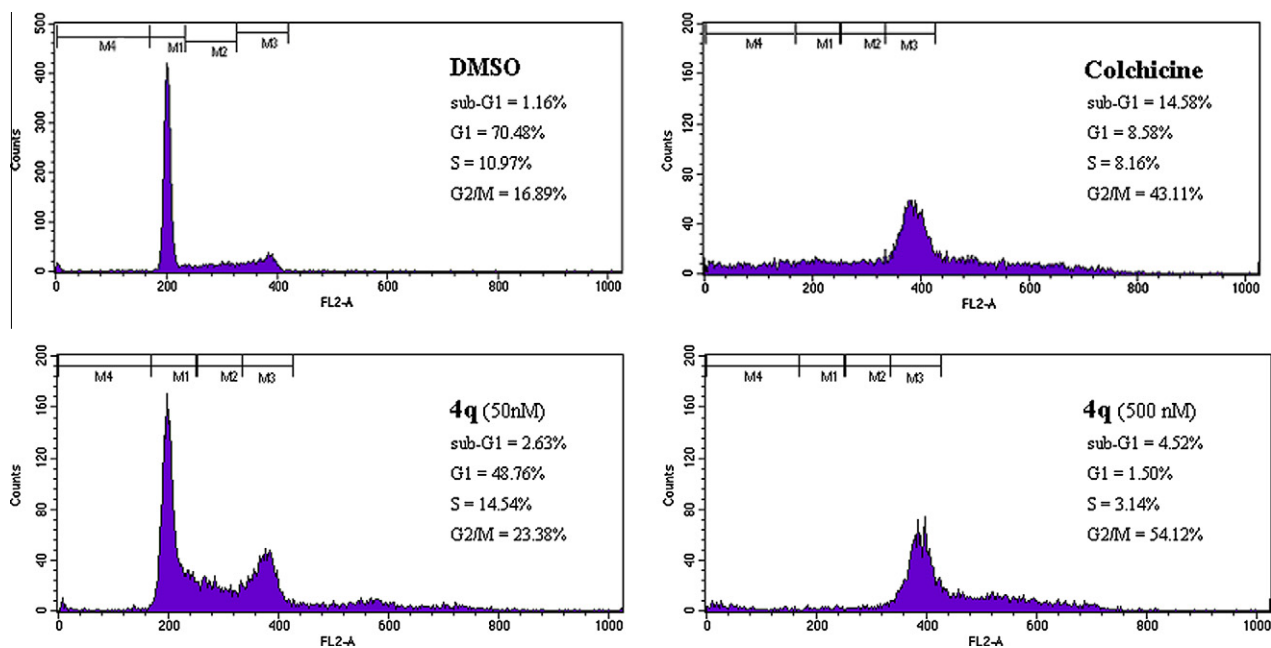


Figure 3. Cell cycle analysis of MCF-7 cells treated with compound **4q** using flow cytometry. Cells were harvested after treatment with **4q** for 24 h and subjected to cell cycle analysis. The percentage of cells in each cell cycle phase was indicated.

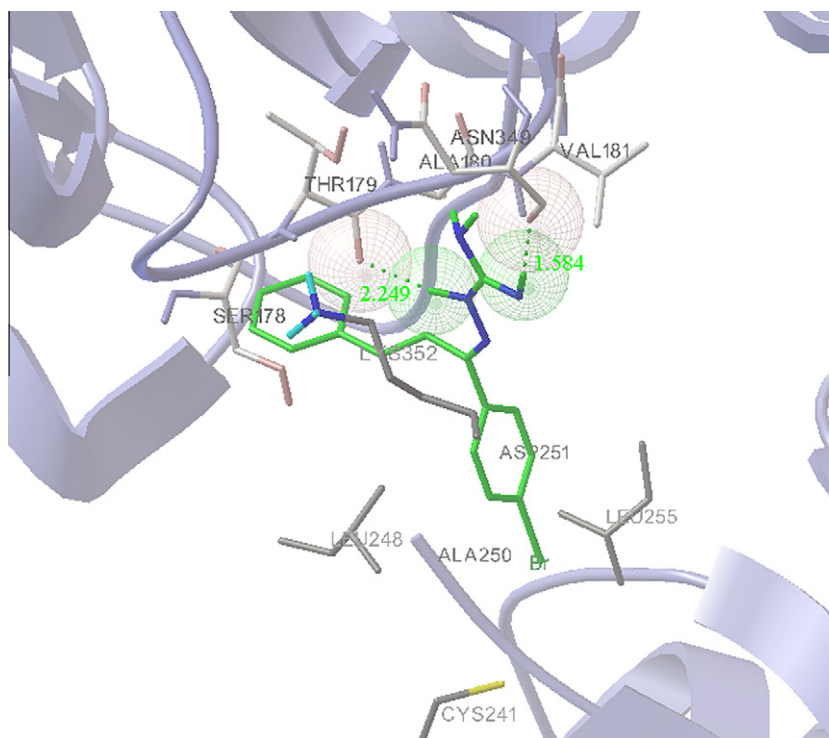


Figure 4A. Compound **4q** (Carbon atom are green) docked into the tubulin pocket. Both side chains of important active site amino acids and hydrogen bonds are shown: THR 179 (angle O...H-N = 146.729°, distance = 2.249 Å), ASN-349 (angle O...H-N = 161.980°, distance = 1.584 Å).

4.5. Antiproliferation assay

The antiproliferative activity of the prepared compounds against MCF-7 human breast carcinoma cells was evaluated as described elsewhere²³ with some modifications. Target tumor cell line was grown to log phase in RPMI 1640 medium supplemented with 10% fetal bovine serum. After diluting to 2×10^4 cells mL⁻¹ with the complete medium, 100 μ L of the obtained cell suspension

was added to each well of 96-well culture plates. The subsequent incubation was permitted at 37 °C, 5% CO₂ atmosphere for 24 h before the cytotoxicity assessments. Tested samples at pre-set concentrations were added to 6-wells with colchicine and CSA-4 co-assayed as positive reference. After 48 h exposure period, 40 μ L of PBS containing 2.5 mg mL⁻¹ of MTT (3-(4,5-dimethylthiazol-2-yl)-2,5-diphenyltetrazolium bromide) was added to each well. Four hours later, 100 μ L extraction solution (10% SDS-5%

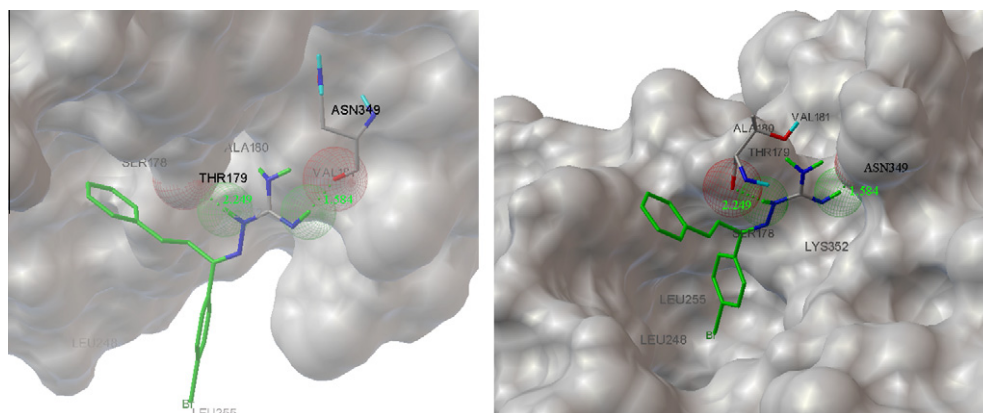


Figure 4B. 3D model of the interaction between compound **4q** and the colchicine binding site. The protein is represented by molecular surface. Compound **4q** is depicted by sticks and balls.

Table 3
Crystallographical and experimental data for compound **4i**

Compounds	4i
Empirical formula	C ₁₆ H ₁₅ ClN ₅ O ₂
Formula weight	344.78
Crystal system	Monoclinic
Space group	P2(1)/n
<i>a</i> (Å)	11.127(2)
<i>b</i> (Å)	11.932(2)
<i>c</i> (Å)	25.889(5)
α (°)	90.00
β (°)	91.71(3)
γ (°)	90.00
<i>V</i> (Å ³)	3435.7(12)
<i>Z</i>	8
<i>D</i> _{calc} (g ⁻¹ cm ⁻³)	1.333
θ range (°)	1.57–25.28
<i>F</i> (0 0 0)	1432
Reflections collected/unique	3126/3120 [<i>R</i> _{int} = 0.0287]
Data/restraints/parameters	3120/0/217
Absorption coefficient (mm ⁻¹)	0.241
<i>R</i> ₁ ; <i>wR</i> ₂ [<i>I</i> > 2σ(<i>I</i>)]	0.0760/0.1817
<i>R</i> ₁ ; <i>wR</i> ₂ (all data)	0.1439/0.2244
GOOF	1.038

isobutyl alcohol–0.01 M HCl) was added. After an overnight incubation at 37 °C, the optical density was measured at a wavelength of 570 nm on an ELISA microplate reader. In all experiments three replicate wells were used for each drug concentration. Each assay was carried out at least three times. The results were summarized in Table 2.

4.6. Effects on tubulin polymerization

Bovine brain tubulin was purified as described previously.²⁴ To evaluate the effect of the compounds on tubulin assembly *in vitro*,²⁵ varying concentrations were preincubated with 10 μM tubulin in glutamate buffer at 30 °C and then cooled to 0 °C. After addition of GTP, the mixtures were transferred to 0 °C cuvettes in a recording spectrophotometer and warmed-up to 30 °C and the assembly of tubulin was observed turbidimetrically. The IC₅₀ was defined as the compound concentration that inhibited the extent of assembly by 50% after 20 min incubation.

4.7. Cell apoptosis morphological assessment by DAPI staining assay

Chromatin condensation was detected by nuclear staining with fluorochrome dye DAPI, this dye can form fluorescent complexes

with natural double-stranded DNA. This method was used to observe the apoptosis morphological changes. Briefly, MCF-7 human breast carcinoma cells were cultured on 6-well plates before treatment. After treatment with 0, 1.0 μM compound **4q** for 24 h, MCF-7 cells were fixed with ice-cold 4% paraformaldehyde for 20 min and washed with ice-cold PBS, then the cell suspension were permeabilized by incubation in 0.1% sodium citrate containing 0.1% Triton X-100 for 2 min at 4 °C and washed with ice-cold PBS, stained with fluorochrome dye DAPI (300 nM). After labeling, samples were observed under a fluorescence microscope.

4.8. Cell cycle assay

MCF-7 human breast carcinoma cells were treated with compound **4q** at 50 nM and 500 nM concentrations for 24 h. Then cells were collected and fixed in 70% cold ethanol (–20 °C) overnight. Cells were resuspended in PBS after washing twice with PBS, RNase A (0.5 mg/mL) and PI (2.5 μg/mL) were then added to the fixed cells for 30 min. The DNA content of cells was then analyzed with flow cytometer.

4.9. Molecular docking modeling

Molecular docking of compound **4q** into the three-dimensional X-ray structure of tubulin (1SA0 PDB, downloaded from the PDB) was carried out using the Auto-Dock software package (version 4.0) as implemented through the graphical user interface Auto-Dock Tool Kit (ADT 1.4.6).

Acknowledgements

The work was financed by a grant (no. BK2009239) from the Jiangsu National Science Foundation.

References and notes

- Valiron, O.; Caudron, N.; Job, D. *Cell. Mol. Life Sci.* **2001**, *58*, 2069.
- Kanthou, C.; Tozer, G. M. *Int. J. Exp. Pathol.* **2009**, *90*, 284.
- Hait, W. N.; Hambley, T. W. *Cancer Res.* **2009**, *69*, 1263.
- De Rycker, M.; Rigoreau, L.; Dowding, S.; Parker, P. J. *Chem. Biol. Drug Des.* **2009**, *73*, 599.
- Jordan, M. A.; Wilson, L. *Nat. Rev. Cancer* **2004**, *4*, 253.
- Carlson, R. O. *Expert Opin. Invest. Drugs* **2008**, *17*, 707.
- Li, W. T.; Hwang, D. R.; Song, J. J.; Chen, C. P.; Chuu, J. J.; Hu, C. B.; Lin, H. L.; Huang, C. L.; Huang, C. Y.; Tseng, H. Y.; Lin, C. C.; Chen, T. W.; Lin, C. H.; Wang, H. S.; Shen, C. C.; Chang, C. M.; Chao, Y. S.; Chen, C. T. *J. Med. Chem.* **2010**, *53*, 2409.
- Andreani, A.; Rambaldi, M.; Leoni, A.; Locatelli, A.; Bossa, R.; Fraccari, A.; Galatulas, I.; Salvatore, G. *J. Med. Chem.* **1996**, *39*, 2852.
- Das, A.; Trousdale, M. D.; Ren, S. J.; Lien, E. J. *Antiviral Res.* **1999**, *44*, 201.

10. Ren, S.; Wang, R.; Komatsu, K.; Patricia, B. K.; Zyrianov, Y.; Mckenna, C. E.; Csipke, C.; Tokes, Z. A.; Lien, E. J. *J. Med. Chem.* **2002**, *45*, 410.
11. (a) Stanek, J.; Caravatti, G.; Capraro, H. G.; Furet, P.; Mett, H.; Schneider, P.; Regenass, U. *J. Med. Chem.* **1993**, *36*, 46; (b) Stanek, J.; Caravatti, G.; Frei, J.; Furet, P.; Mett, H.; Schneider, P.; Regenass, U. *J. Med. Chem.* **1993**, *36*, 2168.
12. (a) Anne, T.; Lien, E. J.; Lai, M. *J. Med. Chem.* **1985**, *28*, 1103; (b) Liu, M.; Lin, T.; Cory, J. G.; Cory, A. H.; Sartorelli, A. C. *J. Med. Chem.* **1996**, *39*, 2586; (c) Ren, S.; Wang, R.; Komatsu, K.; Patricia, B. K.; Zyrianov, Y.; Mckenna, C. E.; Csipke, C.; Tokes, Z. A.; Lien, E. J. *J. Med. Chem.* **2002**, *45*, 410.
13. (a) Andreani, A.; Granaola, M.; Leoni, A.; Locatelli, A.; Morigi, R.; Rambaldi, M.; Lenaz, G.; Fato, R.; Bergamini, C.; Farruggia, G. *J. Med. Chem.* **2005**, *48*, 3085; (b) Andreani, A.; Burnelli, S.; Granaola, M.; Leoni, A.; Locatelli, A.; Morigi, R.; Rambaldi, M.; Varoli, L.; Farruggia, G.; Stefanelli, C.; Masotti, L.; Kunkel, M. W. *J. Med. Chem.* **2006**, *49*, 7897.
14. Nagle, P. S.; Rodriguez, F.; Amila, K.; Quinn, S. J.; Rozas, I. *J. Med. Chem.* **2009**, *52*, 7113.
15. Warrel, R. P., Jr.; Burchenal, J. H. *J. Clin. Oncol.* **1983**, *1*, 52.
16. Zhang, H. Z.; Candace, C. C.; May, C.; Drewe, J.; Tseng, B.; Cai, S. X. *Bioorg. Med. Chem.* **2009**, *17*, 2852.
17. Li, W. T.; Hwang, D. R.; Song, J. S.; Chen, C. P.; Chuu, J. J.; Hu, C. B.; Lin, H. L.; Huang, C. L.; Huang, C. Y.; Tseng, H. Y.; Lin, C. C.; Chen, T. W.; Lin, C. H.; Wang, H. S.; Shen, C. C.; Chang, C. M.; Chao, Y. S.; Chen, C. T. *J. Med. Chem.* **2010**, *53*, 2409.
18. Boumendjel, A.; Boccard, J.; Carrupt, P. A.; Nicolle, E.; Blanc, M.; Geze, A.; Choisnard, L.; Wouessidjewe, D.; Matera, E. L.; Dumontet, C. *J. Med. Chem.* **2008**, *51*, 2307.
19. Jung, J. C.; Jang, S.; Lee, Y.; Min, D.; Lim, E.; Jung, H.; Miyeon, Oh.; Seikwan, Oh.; Jung, M. *J. Med. Chem.* **2008**, *51*, 4054.
20. Lawrence, N. J.; McGown, A. T. *Curr. Pharm. Des.* **2005**, *11*, 1679.
21. Fukumoto, S.; Imamiya, E.; Kusumoto, K.; Fujiwara, S.; Watanabe, T.; Shiraishi, M. *J. Med. Chem.* **2002**, *453*, 3009.
22. Sheldrick, G. M. In *SHELX-97*. Program for X-ray Crystal Structure Solution and Refinement, Göttingen University, Germany, 1997.
23. Boumendjel, A.; Boccard, J.; Carrupt, P. A.; Nicolle, E.; Blanc, M.; Geze, A.; Choisnard, L.; Wouessidjewe, D.; Matera, E. L.; Dumontet, C. *J. Med. Chem.* **2008**, *51*, 2307.
24. Hamel, E.; Lin, C. M. *Biochemistry* **1984**, *23*, 4173.
25. Hamel, E. *Cell Biochem. Biophys.* **2003**, *38*, 1.